sciendo
ISSN 1335-8871
MEASUREMENT SCIENCE REVIEW
Journal homepage: https://content.sciendo.com

The Importance of ECG Offset Correction for Premature Ventricular Contraction Origin Localization from Clinical Data

Jana Svehlikova[1], Anna Pribilova[1], Jan Zelinka[1], Beata Ondrusova[1,3], Katarina Kromkova[2], Peter Hlivak[2], Robert Hatala[2], Milan Tysler[1]

[1]*Institute of Measurement Science, Slovak Academy of Sciences, Department of Biomeasurements, Dubravska cesta 9, 84104 Bratislava, Slovakia, jana.svehlikova@savba.sk*
[2]*National Institute for Cardiovascular Diseases, Department of Arrhythmias and Cardiostimulation, Pod Krasnou horkou 1, 83348 Bratislava, Slovakia*
[3]*Faculty of Electrical Engineering and Information Technology, Slovak University of Technology in Bratislava, Ilkovičova 2961, 841 04 Bratislava, Slovakia*

Abstract: In this study, the inverse solution with a single dipole was computed to localize the premature ventricular contraction (PVC) origin from long term multiple leads ECG measurements on fourteen patients. The stability of the obtained results was studied with respect to the preprocessing of signals used as an input to the inverse solution and the complexity of the torso model. Two methods were used for the baseline drift removal. After an averaging of the heartbeats, the influence of the retention or elimination of the remaining offset at the beginning of the PVC signal was examined. The inverse computations were performed using both homogeneous and inhomogeneous patient-specific torso models. It was shown that the remaining offset in the averaged signals at the beginning of the PVC signal had the most significant impact on the stability of the resulting position within the ventricles. Its elimination stabilizes the location of the results, decreases the sensitivity to the torso model complexity and decreases the sensitivity to the primary baseline drift removal method. The additional offset correction decreased the mean distance between the results for all patients from 17-18 mm to 1-2 mm, regardless of the baseline drift removal method or the torso model complexity.

Keywords: Body surface potential mapping, inverse solution, ECG signal processing, QRS beginning assessment, signal offset.

1. INTRODUCTION

Since the mechanical activity of the ventricles is preceded and controlled by their electrical excitation, the measured ECG signals reflect the heart function. Body surface potential mapping is one of the advanced techniques to obtain information about the patient's heart condition when the ECG signals are measured in tens of electrodes instead of the nine used in conventional ECG examinations. Such complex multiple-leads ECG measurement allows the mathematical expression of the relations between the cardiac generator and the body surface potentials used for the so-called inverse solutions of electrocardiography or electrocardiographic imaging (ECGI). The main goal of the solution of the inverse problem of electrocardiography is to examine the heart function noninvasively [1] and help in preoperation planning of the invasive interventions, especially for an elimination of the origins of ventricular or atrial arrhythmias [2], [3], [4]. Besides the multiple-leads ECG measurement, the inverse solution requires a patient-specific torso model with a known heart geometry and positions of electrodes on the chest. Such a model is created from CT or MR images of the patient's thorax. More complex inhomogeneous torso models also include the lungs and heart cavities [5], [6].

There are several approaches for solving the inverse problem regarding the computational method [7], [8], [9], as well as the equivalent electrical generator [10]. In general, the inverse problem leads to a solution to the ill-posed system of linear equations. Therefore, regularization methods are used to obtain a unique result with physiological meaning [11], [12]. Usually, zero-order or second-order Tikhonov regularization is applied.

In this study, the equivalent heart generator is assumed in the form of a single dipole which can represent local changes in the activation of the heart volume. This approach was used for the localization of small ischemic lesions in the ventricles [13], [14] and also for the localization of undesired premature ventricular activity [15]. The methods were studied mainly on simulated data or data obtained during experiments with animal hearts in the torso tank [16], so the signals were not measured from real human objects. Theoretically, the ECG signals are quasi-periodical, and the morphology of corresponding normal or pathological beats should be the

DOI: 10.2478/msr-2022-0031

same. However, it is well known that the heart cycles are affected by some intraindividual variability as well as by breathing and other factors. Therefore, the representative heart signal is chosen from many heart cycles obtained by a signal averaging technique [17] to get more common information about the heart cycles.

It was shown in a recent paper [18] that proper signal processing plays an essential role in obtaining the correct inverse result. The aim of the presented work was to study the importance of the final signals' offset correction (just before their use in the inverse procedure) for the results of the premature ventricular contraction (PVC) localization by a single dipole applied to clinical data.

2. SUBJECT & METHODS

A. Patients and measurements

In cooperation with the National Institute for Cardiovascular Diseases in Bratislava, fourteen patients with detected PVCs and indicated for the radiofrequency ablation procedure underwent additional body surface potential (BSP) mapping measurement to obtain the data for noninvasive localization of their PVC origin. Each patient was informed about the measurement and signed the informed consent to the procedure. All obtained data were anonymized for later processing.

The BSP mapping was performed by the ProCardio multichannel measuring system [19] developed in our laboratory. One hundred twenty-eight (128) disposable electrodes were placed on the torso and three electrodes were placed in the standard limb-leads positions. Additional two electrodes were used as a common mode sense (CMS) electrode and an active grounding (driven right leg, DRL) electrode. The torso electrodes were organized in strips, with eight electrodes in each strip placed vertically on the torso/chest. Together, all electrodes placed on the torso of each patient created approximately a grid 8 by 16 electrodes, as is visible in Fig.1. left. The duration of the measurements varied from 5 to 20 minutes. The signals were recorded with a sampling frequency of 1 kHz.

After the body surface potential mapping, each patient was sent for a CT scan while the strips with the electrodes remained stuck on the patient's torso. The personalized torso model needed for the inverse solution was created from the obtained CT images in which also the precise positions of the measuring electrodes were displayed. The volumes of selected internal organs were segmented by contouring using the Tomocon software [20]. The inhomogeneous torso model consisted of the torso with electrode positions, the lung lobes, and the left and right cardiac cavities (atria and ventricles) together with initial parts of the main arteries – the aorta and pulmonary artery (Fig.1. right). The closed volume around both ventricles was also defined. The mass of the ventricular myocardium was computed by subtraction of the ventricular cavities from the closed volume around the ventricles and later exported as a closed endo-epicardial surface along with the closed triangulated surfaces of other organs. In the homogeneous torso model, only endo-epicardial and torso surfaces were considered.

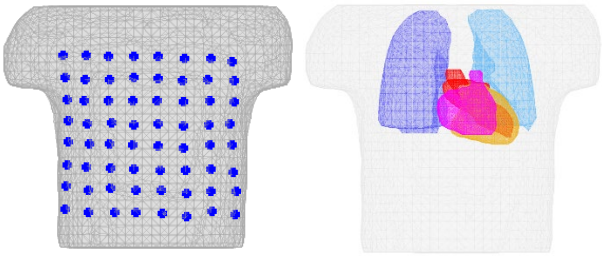

Fig.1. Left: The measuring electrodes' position on the frontal part of the patient's torso. Right: Inhomogeneous patient-specific torso model.

B. ECG signal processing

The first step in the processing of the measured long term ECG signals was the baseline drift removal (BDR). Two BDR methods were used:

Cubic spline (CS) method: the zero points with assumed zero potential value were defined before the P-wave of each normal/sinus beat according to the physiological properties of ECG signal with sinus rhythm. Then, the zero line was estimated by a cubic spline using the estimated zero points during the measurement. The baseline drift of the signal was eliminated by subtraction of the zero line from the measured raw signal.

High pass filter (HP) method: the baseline drift/wandering was eliminated using a high-pass filter with the finite impulse response designed by the window method and the Blackman-Harris window [21] for its very good side-lobe attenuation. The cut-off frequency of the filter was chosen as 0.5 Hz for 6-dB attenuation of the magnitude frequency response, and the filter order was chosen as ten times the sampling frequency in Hz, giving the delay of 5 s.

The R-peaks of the cardiac cycles were found in the standard lead II by the Pan-Tompkins method [22] and were used as the reference time points for each cardiac cycle. The studied time interval was defined as 220 ms before the R-peak and 330 ms after it. This time window covered the QRS interval for both normal as well as PVC beats. The morphology of the heartbeats in the signal was distinguished by the k-means clustering method [23]. A criterion function for clustering was an L2 norm of the difference between two signals during the studied time window. In each cluster, an averaged signal from all cluster members was computed. Then, the averaged signals with PVC morphology were used for the computation of body surface potential maps (BSPMs), which later served as the input data for an inverse problem solution to find the origin of the PVC activity.

It was found that after both BDR methods mentioned above, some offset remained in the signals at the beginning of the averaged PVC heartbeat. Therefore, the additional offset correction (OFC) was applied. The beginning of the PVC was estimated manually from three signals: the II standard limb lead, the precordial lead 36 corresponding with the standard lead V2, and the root-mean-squared signal from all leads. In each lead, the whole course of the averaged signal was shifted by the corresponding constant value in this time instant so that the BSPM in the beginning of the PVC was set to zero (Fig.2.).

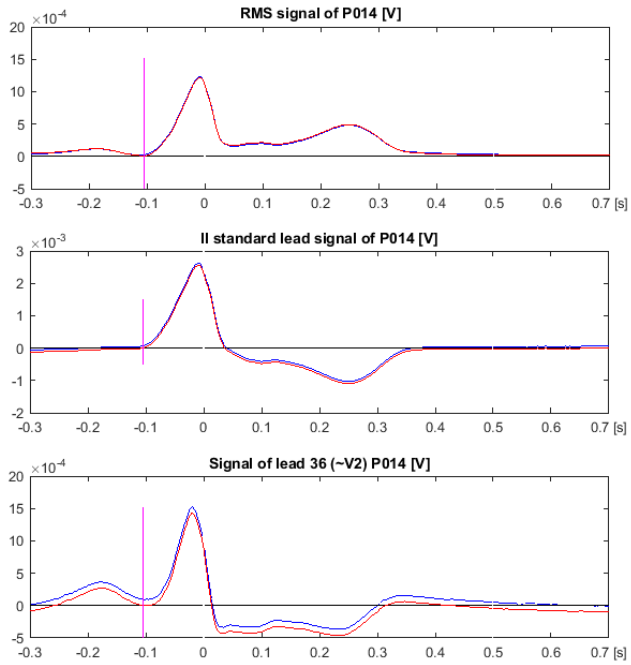

Fig.2. Example of the additional correction of the remaining offset at the beginning of the averaged PVC beat. Blue – original signal, red - corrected signal, vertical line denotes the estimated beginning of the PVC depolarization.

The influence of such additional signal correction on the position of the inverse result was examined. Therefore, the inverse solution for each patient was computed for eight combinations of the torso model and signal processing method:

- NOFC CS hom: CS BDR method, homogeneous torso model (hom), no additional offset correction (NOFC);
- NOFC CS inh: CS BDR method, inhomogeneous torso model (inh), no additional offset correction;
- NOFC HP hom: HP BDR method, homogeneous torso model, no additional offset correction;
- NOFC HP inh: HP BDR method, inhomogeneous torso model, no additional offset correction;
- OFC CS hom: CS BDR method, homogeneous torso model, with additional offset correction (OFC);
- OFC CS inh: CS BDR method, inhomogeneous torso model, with additional offset correction;
- OFC HP hom: HP BDR method, homogeneous torso model, with additional offset correction;
- OFC HP inh: HP BDR method, inhomogeneous torso model, with additional offset correction.

C. *Inverse solution*

The inverse solution was studied in the form of a single dipole as it is introduced in [13]. The identification of the position and moments of a single dipole as the equivalent cardiac generator leads to the so-called "moving dipole" problem [24], which is nonlinear and can be solved iteratively. However, for the known/defined position of the dipole, the problem turns linear and can be solved directly. So that, an a priori knowledge that the location of the resulting dipole should be within the volume of ventricular myocardium is used in the inverse solution. In this study, the equivalent dipole was computed for predefined positions on the endo-epicardial surface of the ventricles.

For a defined position of the dipole, the corresponding map of electrical potentials dip_map on the torso model can be computed as:

$$dipMap = \boldsymbol{T}d, \tag{1}$$

where $\boldsymbol{T}$ is a transfer matrix computed by a boundary element method in a torso model, describing the relation between the dipole d in the given position and the potentials on the torso that is assumed as a volume conductor. It can be either homogeneous with a constant electrical conductivity inside the volume or inhomogeneous when additional volumes of lung lobes and heart cavities are taken into account with a different electrical conductivity. With respect to the torso conductivity, the conductivity of the lungs is assumed as four times lower and the conductivity of the cavities three times higher. The whole torso is surrounded by a non-conductive medium.

Considering (1) a computation of dipole moments from a measured BSPM leads to:

$$d = \boldsymbol{T}^{-1}BSPM. \tag{2}$$

From (2), for any given position of the dipole, only three dipole moments are studied, i.e., it is an overdetermined linear system that can be solved by the minimal least-squares method.

The main assumption of searching the PVC origin using a single dipole is that in premature ventricular activity, the activation starts in a single small region, thus at the beginning of depolarization, the activated area is so small that an equivalent electrical generator of such region can be approximated by a single dipole. Therefore, the inverse solution using a single dipole for a PVC origin localization is computed from the measured BSPMs from the initial 30 ms of the PVC cycle.

For each position i on the endo-epicardial surface and *BSPM(t)* in each time step t∈<1,30> a dipolar moment *d(i,t)* is computed according to (2), and a corresponding map *dipMap(i,t)* according to (1). The quality of the similarity of the input BSPM and the map computed from the estimated inverse dipole is evaluated by the relative residual error parameter (RRE), calculated for each time step and dipole position as:

$$RRE(i,t) = \|BSPM(t) - dipMap(i,t)\| \,/\, \|BSPM(t)\|, \tag{3}$$

where ||.|| means the Euclidean norm.

Then the position of the inverse dipole *d(i,t)* producing *dipMap(i,t)* giving a minimal *RRE(i,t)* in the studied initial time interval is the best representative of the input *BSPM*, thus assumed as the position of the PVC origin.

3. RESULTS

A. *Patients and measurements*

The average age of the fourteen patients was 52 years (from 17 to 79); out of them were three women and 11 men. The number of processed and averaged PVC beats for one patient varied from 4 to 616 (average 191, median 168).

B. ECG signal processing

For each patient, from the measured BSPMs, the PVC beats were clustered according to their morphology by a k-means algorithm in each out of the 128 leads. Then in each lead, the signals in the cluster with PVC beats were averaged, and the representative measured PVC beat was created. The BSPM from averaged PVC signals was used as an input for the inverse computation according to (2).

The beginning of the PVC beat was estimated manually, inspecting a root-mean-squared (RMS) signal from all leads together with the II standard lead and lead number 36 corresponding to the standard precordial lead V2. For the additional offset correction, the whole signal was shifted by the value at the estimated beginning of the PVC so that the PVC beat started at zero value in all leads, as it is shown in Fig.2.

In each lead, a different value of the offset at the estimated beginning of the PVC signal remained. The average value of the offsets for 128 leads (mean) and the difference between maximal and minimal value (range) in 128 leads for each patient and for the two BDR methods are summarized in Table 1.

Table 1. The average value and the range (max-min) of the offsets in 128 leads for each patient.

Patient	mean HP [μV]	range HP [μV]	mean CS [μV]	range CS [μV]
P01	7.0	128.8	3.6	195.1
P02	-1.4	143.2	23.3	220.4
P04	5.3	55.6	3.6	76.4
P06	-1.3	43.2	8.2	157.2
P08	-16.7	191.3	7.4	238.3
P10	12.0	144.4	14.2	144.6
P14	2.3	171.9	4.3	226.9
P20	10.7	129.7	15.9	231.7
P21	-9.5	107.6	2.7	38.4
P23	2.8	31.5	10.6	95.8
P24	12.6	24.7	7.0	83.0
P27	1.5	42.0	-1.8	87.6
P29	-1.2	45.5	-1.2	76.2
P36	-2.0	47.5	10.8	93.6

As it is mentioned in the Methods, in the inverse solution, the best dipole $d(i,t)$ representing the PVC origin and producing the most similar $dipMap(i,t)$ to the measured $BSPM(t)$ is characterized by the minimal value of the $RRE(i,t)$ parameter within the initial time interval <1,30> ms of the PVC beat. The influence of the used combination of the torso model and the signal processing method on the minimal $RRE(i,t)$ parameter can be observed in Fig.3.

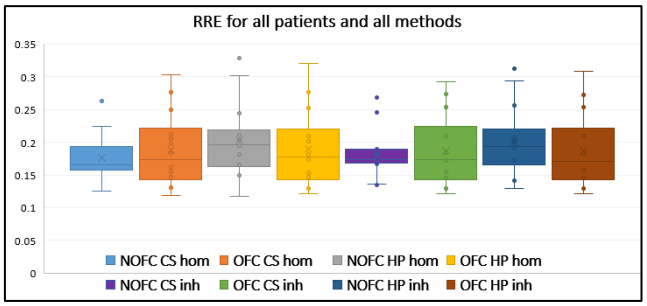

Fig.3. Relative residual error of the inverse solution for all patients in dependence on the BDR, torso model and NOFC or OFC signal processing.

C. Inverse solution

Next, the impact of the OFC on the stability of the inverse solution was studied.

The positions of the inverse results depended on whether the OFC was applied or not (NOFC). The distances between the results for NOFC and OFC for all patients and the same BDR method and torso model are depicted in Fig.4.

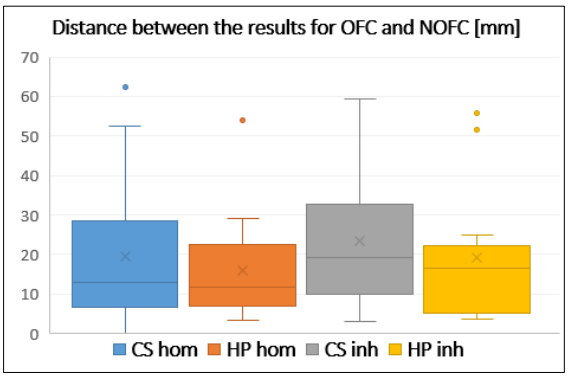

Fig.4. Distances between the inversely estimated positions of the PVC origin for all patients and for NOFC and OFC processed signals in dependence on the BDR and torso model.

Regarding the torso model, we observed the distances between the inverse results for the same patient with respect to the BDR and the OFC/NOFC signal processing method, as it is summarized in Fig.5.

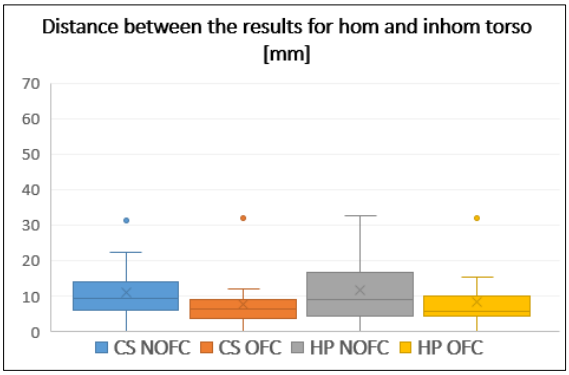

Fig.5. The influence of the used torso model on the inverse results for all patients and the two BDR methods and NOFC or OFC signal processing, respectively.

Finally, the stability of the results using both BDR methods was studied in dependence on the NOFC/OFC signal processing. For each patient, differences between the inverse results for CS and HP BDR methods were evaluated for NOFC and OFC signal processing, as is visualized in Fig.6.

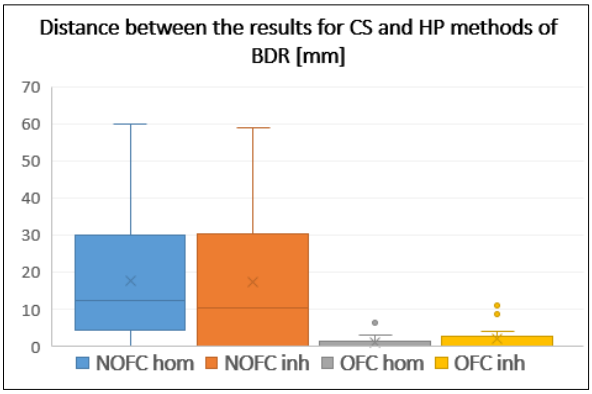

Fig.6. Distances between the inverse results for CS and HP BDR methods for NOFC/OFC signal processing and homogeneous and inhomogeneous torso model.

4. Discussion and Conclusions

The inverse solution using a single dipole to identify the origin of the undesired ventricular activity from ECG signals is computed from the very short time interval of 30 ms after the beginning of the PVC. Results of the presented study suggest that the used method can be very sensitive to careful preprocessing of the ECG signals before the inverse solution computation.

As we can see from Fig.4., the average distance between the inverse results computed for input signals with and without the additional offset correction is about 20 mm (from 16 to 23 mm), which is a considerably significant value and does not depend on the complexity of the torso model or BDR method.

In Fig.5. a lower influence of the torso model on the positions of the inverse results can be observed when the average distance of the inverse results in dependence on the torso model is about 8 mm if the OFC signal processing is performed. Without OFC, the influence of the torso model causes the average distance between the inverse results for a patient to be more than 11 mm.

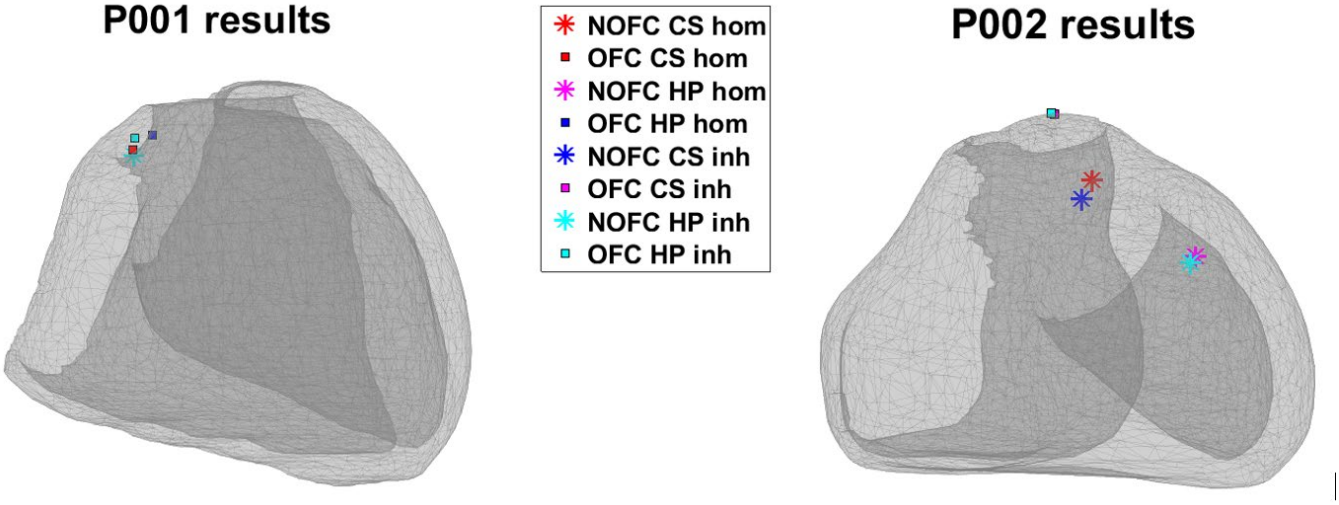

Fig.7. Examples of stability of the obtained inverse results for the studied eight combinations of the torso model and signal processing method. The legend is the same for both pictures.

The importance of the offset correction in each lead of the measured BSPM before the inverse problem computation is the most remarkable in Fig.6. For NOFC signals used as the input for the inverse solution, the results are ambiguous and very sensitive to the BDR method. The average distance between the results for one patient is 17 or 18 mm. After OFC signal processing, the average distance between the inverse results in dependence on homogeneous or inhomogeneous torso model decreases rapidly to 1 or 2 mm, respectively. Hence, both BDR methods lead to very similar results and can be considered equal. However, the use of the cubic spline method needs a subjective decision of the observer to define the zero point correctly before the P-wave of the normal/sinus ECG signal for each patient. High-pass filtering works without a subjective intervention, but on the other hand, the filter should be appropriately designed in advance.

In three out of fourteen patients, the position of inversely estimated PVC origin was not influenced by the presented signal processing methods or torso models, as is illustrated in Fig.7. left. However, in most cases, ignoring the proper estimation and correction of the ECG signal led to ambiguous results, as shown in Fig.7. right.

As it is apparent from the results for signals without additional offset correction (Fig.4. to Fig.7.), the inversely estimated positions of PVC origin showed a large ambiguity regarding the primary baseline correction method or torso complexity, so they could not be considered reliable. Therefore, we focused mainly on the signal processing

method leading to stable results in this study. Concerning the position of applied radiofrequency ablation (RFA) or the most premature ventricular activity measured for specific patients, we have only verbal descriptions provided by the physicians so far. Of the 14 patients involved in the study, the position of the PVC origin was 5 times in the right ventricular outflow tract (RVOT), 4 times in the left ventricular outflow tract (LVOT), 3 times near the His bundle, one was in the anterior left ventricular (LV) wall and one patient was ablated unsuccessfully. Three patients with the PVC origin near the His bundle were not ablated, only their activation times were measured during an intraventricular mapping procedure, and the earliest activation localization was identified by physicians. From these three patients, the inverse results with OFC showed the correct position for two of them; the third patient had the PVC origin position located inferiorly in the left ventricle. For patients with PVC origin position in RVOT, in four cases, the OFC results showed the RVOT location correctly; however, in two cases, not on the right side of the opening. In one case (incorrect), the inverse results were displayed on the left ventricle anterior. For patients with PVC origin position in the LVOT or the left ventricle, all inverse results for OFC signals correctly showed the LV; in one case, the result was located on the LV free wall instead of near LVOT.

In the future study, we intend to increase the number of patients and export and process the geometrical data from the used electrophysiological mapping systems for better evaluation of the localization error of the inverse method.

The beginning of the PVC signal was estimated manually in this study. We used a single time instant for the offset value from the averaged signal; thus, we assumed the high frequency (HF) noise was eliminated by the averaging. However, this is not the case if the number of PVC signals is small. Of fourteen datasets used in this study, there were two with a number of beats less than 10 (4,9). In all other datasets, there were more than 30 beats, and in nine of them, the number of beats was more than 100. There was not a large HF noise in the data, so we did not consider its additional elimination. Still, in general, this point should be taken into consideration, mainly if the number of measured PVC beats is less than 10.

In the presented study, we focus on the additional offset correction as such, whether it is worth doing it or not. The sensitivity of this approach to HF noise and subjective selection of the PVC starting time instant can be explored in future work. Next, the use of automatic detection of depolarization beginning such as [25] can be examined in the future to speed up and automate the signal processing procedure.

From the results, we can conclude that the proper ECG signal processing, including the additional subtraction of the offset in each measured lead at the beginning of the investigated PVC beat, is essential for obtaining stable inverse localization of the PVC origin.

ACKNOWLEDGMENT

This work was supported by the research grant 2/0109/22 from the VEGA Grant Agency in Slovakia and by grants APVV-14-0875 and APVV-19-0531 from the Slovak Research and Development Agency.

REFERENCES

[1] Cluitmans, M.J.M., Peeters, R.L.M., Westra, R.L., Volders, P.G.A. (2015). Noninvasive reconstruction of cardiac electrical activity: Update on current methods, applications and challenges. *Netherlands Heart Journal*, 23 (6), 301–311. https://doi.org/10.1007/s12471-015-0690-9

[2] Zhou, S., Sapp, J.L., AbdelWahab, A., Šťovíček, P., Horáček, B.M. (2018). Localization of ventricular activation origin using patient-specific geometry: Preliminary results. *Journal of Cardiovascular Electrophysiology*, 29 (7), 979–986. https://doi.org/10.1111/jce.13622

[3] Van Dam, P.M., Tung, R., Shivkumar, K., Laks, M. (2013). Quantitative localization of premature ventricular contractions using myocardial activation ECGI from the standard 12-lead electrocardiogram. *Journal of Electrocardiology*, 46 (6), 574–579. https://doi.org/10.1016/j.jelectrocard.2013.08.005

[4] Guillem, M.S., Climent, A.M., Rodrigo, M., Hernandez-Romero, I., Liberos, A., Fernandez-Aviles, F., Berenfeld, O., Atienza, F. (2016). Noninvasive identification of atrial fibrillation drivers: Simulation and patient data evaluation. *Computing in Cardiology*, 43, 121–124. http://dx.doi.org/10.22489/CinC.2016.039-420

[5] Zemzemi, N., Dobrzynski, C., Bear, L.R., Potse, M., Dallet, C., Coudiere, Y., Dubois, R., Duchateau, J. (2015). Effect of the torso conductivity heterogeneities on the ECGI inverse problem solution. *Computing in Cardiology*, 42, 233–236. http://dx.doi.org/10.1109/cic.2015.7408629

[6] Punshchykova, O., Švehlíková, J., Tyšler, M., Grünes, R., Sedova, K., Osmančík, P., Žďárská, J., Heřman, D., Knepp, P. (2016). Influence of torso model complexity on the noninvasive localization of ectopic ventricular activity. *Measurement Science Review*, 16 (2), 96–102. https://doi.org/10.1515/msr-2016-0013

[7] Zhou, S., Sapp, J.L., Dawoud, F., Horacek, B.M. (2019). Localization of activation origin on patient-specific epicardial surface by empirical Bayesian method. *IEEE Transactions on Biomedical Engineering*, 66 (5), 1380–1389. https://doi.org/10.1109/tbme.2018.2872983

[8] Onak, O.N., Serinagaoglu Dogrusoz, Y., Weber, G.W. (2018). Effects of a priori parameter selection in minimum relative entropy method on inverse electrocardiography problem. *Inverse Problems in Science and Engineering*, 26 (6), 877–897. https://doi.org/10.1080/17415977.2017.1369979

[9] Serinagaoglu Dogrusoz, Y. (2019). Statistical estimation applied to electrocardiographic imaging. In *2019 12th International Conference on Measurement*. IEEE, 2-9. https://doi.org/10.23919/MEASUREMENT47340.2019.8779856

[10] Schuler, S., Schaufelberger, M., Bear, L.R., Bergquist, J.A., Cluitmans, M.J.M., Coll-Font, J., Onak, O.N., Zenger, B., Loewe, A., MacLeod, R.S., Brooks, D.H., Doessel, O. (2022). Reducing line-of-block artifacts in

cardiac activation maps estimated using ECG imaging: A comparison of source models and estimation methods. IEEE *Transactions on Biomedical Engineering*, 69 (6), 2041-2052. http://dx.doi.org/10.1109/TBME.2021.3135154

[11] Zhang, Y., Ghodrati, A., Brooks, D.H. (2005). An analytical comparison of three spatio-temporal regularization methods for dynamic linear inverse problems in a common statistical framework. *Inverse Problems*, 21 (1), 357–382. http://dx.doi.org/10.1088/0266-5611/21/1/022

[12] Tuboly, G., Kozmann, G., Maros, I. (2015). Computational aspects of electrocardiological inverse solutions. *IFAC-PapersOnLine*, 48 (20), 48–51. https://doi.org/10.1016/j.ifacol.2015.10.113

[13] Tysler, M., Svehlikova, J. (2013). Noninvasive finding of local repolarization changes in the heart using dipole models and simplified torso geometry. *Journal of Electrocardiology*, 46 (4), 284–288. https://doi.org/10.1016/j.jelectrocard.2013.03.014

[14] Svehlikova, J., Teplan, M., Tysler, M. (2015). Noninvasive identification of two lesions with local repolarization changes using two dipoles in inverse solution simulation study. *Computers in Biology and Medicine*, 57, 96–102. https://doi.org/10.1016/j.compbiomed.2014.11.020

[15] Svehlikova, J., Teplan, M., Tysler, M. (2018). Geometrical constraint of sources in noninvasive localization of premature ventricular contractions. *Journal of Electrocardiology*, 51 (3), 370-377. https://doi.org/10.1016/j.jelectrocard.2018.02.013

[16] Svehlikova, J., Zelinka, J., Dogrusoz, Y.S., Good, W., Tysler, M., Bear, L. (2018). Impact of signal preprocessing on the inverse localization of the origin of ventricular pacing. *Computing in Cardiology*, 45, 3–6. https://doi.org/10.22489/CinC.2018.315

[17] Tan, N., Bear, L., Potse, M., Puyo, S., Meo, M., Dubois, R. (2019). Analysis of signal-averaged electrocardiogram performance for body surface recordings. *Computing in Cardiology*, 45, 3–6. https://doi.org/10.23919/CinC49843.2019.9005816

[18] Bear, L.R., Dogrusoz, Y.S., Good, W., Svehlikova, J., Coll-Font, J., Van Dam, E., MacLeod, R. (2021). The impact of torso signal processing on noninvasive electrocardiographic imaging reconstructions. *IEEE Transactions on Biomedical Engineering*, 68 (2), 436–447. https://doi.org/10.1109/TBME.2020.3003465

[19] Kadanec, J. Zelinka, J. Bukor, G. Tysler, M. (2017). ProCardio 8 - System for high-resolution ECG mapping. In *2017 11th International Conference on Measurement*. IEEE, 263–266. https://doi.org/10.23919/MEASUREMENT.2017.7983586

[20] TatraMed Software. https://tatramed.sk/tomocon-workstation/

[21] Harris, F.J. (1978). On the use of windows for harmonic analysis with the discrete Fourier transform. *Proceedings of the IEEE*, 66 (1), 51–83. https://doi.org/10.1109/PROC.1978.10837

[22] Pan, J., Tompkins, W.J. (1985). A real-time QRS detection algorithm. *IEEE Transactions on Biomedical Engineering*, 32 (3), 230–236. https://doi.org/10.1109/TBME.1985.325532

[23] Bishop, C.M. (2006). K-means clustering. In *Pattern Recognition and Machine Learning*. Springer, 424–430. ISBN 978-0387310732.

[24] Oostendorp, T., Van Oosterom, A. (1989). Source parameter estimation in inhomogeneous volume conductors of arbitrary shape. *IEEE Transactions on Biomedical Engineering*, 36 (3), 382–391. https://doi.org/10.1109/10.19859

[25] Bae, T.W., Kwon, K.K. (2021). ECG PQRST complex detector and heart rate variability analysis using temporal characteristics of fiducial points. *Biomedical Signal Processing and Control*, 66, 102291. https://doi.org/10.1016/j.bspc.2020.102291

Received January 23, 2022
Accepted May 30, 2022